

Spectral analysis for elastica 3-dimensional dynamics in a shear flow

Lujia Liu, Paweł Sznajder, and Maria L. Ekiel-Jeżewska*
*Institute of Fundamental Technological Research,
 Polish Academy of Sciences, Pawińskiego 5b, 02-106 Warsaw, Poland*
 (Dated: July 14, 2023)

We present the spectral analysis of three-dimensional dynamics of an elastic filament in a shear flow of a viscous fluid at a low Reynolds number in the absence of Brownian motion. The elastica model is used. The fiber initially is almost straight at an arbitrary orientation, with small perpendicular perturbations in the shear plane and out-of-plane. To analyze the stability of both perturbations, equations for the eigenvalues and eigenfunctions are derived and solved by the Chebyshev spectral collocation method. It is shown that their crucial features are the same as in case of the two-dimensional elastica dynamics in shear flow [Becker and Shelley, Phys. Rev. Lett. 2001] and the three-dimensional elastica dynamics in the compressional flow [Chakrabarti et al., Nat. Phys., 2020]. We find a similar dependence of the buckled shapes on the ratio of bending to hydrodynamic forces as in the simulations for elastic fibers of a nonzero thickness [Slowicka et al., New J. Phys., 2022].

I. INTRODUCTION

Dynamics of flexible micro and nano-objects in fluid flows have been recently widely investigated theoretically, numerically, and experimentally [1–3]. The interest is motivated by potential applications to microorganisms (e.g., diatoms [4], bacteria [5], cells [6] or actin [7, 8]), and to artificially produced micro and nanofibers [9, 10].

For elastic filaments, typical time-dependent shape deformations and orientations have been analyzed for different values of the bending stiffness and aspect ratio. Buckling of elastic filaments has been studied in various fluid flows: extensional [5, 11, 12], cellular [13–16], stagnation point [17], corner [18], shear [19–21], and unidirectional [22].

Many articles have focused on flexible filaments in shear flows [4, 6–8, 23–30]. The buckling instability of slender fibers located in the shear plane has been derived from the 2-dimensional spectral analysis of the elastica [21]. The eigenvalues have been evaluated for a wide range of values of the elastoviscous number [21].

The goal of this work is to analyze the stability of elastica in a shear flow by solving a 3-dimensional spectral problem: not only for in-plane but also for out-of-plane perturbations. Using the Chebyshev collocation method [31], we evaluate the eigenvalues and eigenfunctions and discuss the results.

II. SYSTEM AND THEORETICAL MODEL

A. Elastica 3-dimensional equation

A slender elastic filament is immersed in a shear flow $\tilde{U} = (\dot{\gamma}y, 0, 0)$ of a fluid with the dynamic viscosity μ . The ratio of the radius R of the particle cross-section to its

length L is much smaller than unity, i.e., $R/L \ll 1$. The filament is assumed to be inextensible, and its length L is used as the unit of length. The dimensionless position of the filament centerline is denoted as $\mathbf{x}(s, t)$, where $s \in [-1/2, 1/2]$ is the arclength coordinate of a filament segment and t is time. Owing to the filament inextensibility, $\mathbf{x}_s \cdot \mathbf{x}_s = 1$. Here we ignore gravitational effects, Brownian forces, and fluid inertia, assuming that the Reynolds number is much smaller than unity; only elastic and viscous forces are considered to result in the filament dynamics following from the Stokes equations. The slender body approximation [32] is used. With the length unit L , the time unit $\dot{\gamma}^{-1}$ and $\mathbf{U} = \tilde{U}/(\dot{\gamma}L)$, the dimensionless elastica 3D governing equation is [1, 17, 21, 33, 34],

$$\eta(2\mathbf{I} - \mathbf{x}_s \mathbf{x}_s) \cdot (\mathbf{x}_t - \mathbf{U}(\mathbf{x})) = (T(s, t)\mathbf{x}_s)_s - \mathbf{x}_{ssss}, \quad (1)$$

where $\eta = \frac{2\pi\mu\dot{\gamma}L^4}{EI \ln(L/R)}$ denotes the ratio of the viscous drag to the elastic restoring forces [17], E is the Young's modulus of the filament and $I = \pi R^4/4$ is the area moment of inertia. Here $T(s, t)$ represents the tension in the filament at point s and time t .

The particle is slightly deformed from a straight shape at a certain orientation, described by the azimuthal and polar angles, $\phi(t)$ and $\theta(t)$, as shown in Fig. 1. The

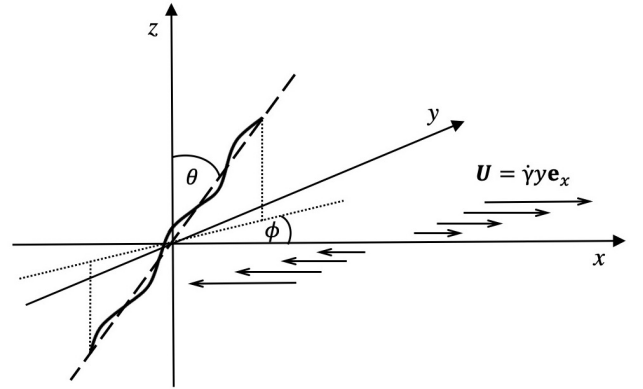


FIG. 1: A schematic of a slender particle in a shear flow.

*Corresponding author. Email: mekiel@ippt.pan.pl

azimuthal angle deals with the projection onto the shear plane (x, y) . Owing to symmetries, we can restrict to $0 \leq \phi \leq \pi$ and $0 \leq \theta \leq \pi/2$ without loss of generality.

The position vector $\mathbf{x}(s, t)$ can be described by

$$\mathbf{x} = s\boldsymbol{\lambda} + u\boldsymbol{\lambda}_i + v\boldsymbol{\lambda}_o, \quad (2)$$

where u and v are respectively the in-plane and out-of-plane deflections relative to a straight rod with the orientation determined by the unit vector $\boldsymbol{\lambda} = (\cos \phi \sin \theta, \sin \phi \sin \theta, \cos \theta)$. Here $\boldsymbol{\lambda}_i = (-\sin \phi, \cos \phi, 0)$ denotes the in-plane (x, y) unit vector perpendicular to $\boldsymbol{\lambda}$ and $\boldsymbol{\lambda}_o = (-\cos \phi \cos \theta, -\sin \phi \cos \theta, \sin \theta)$ denotes the out-of-plane unit vector perpendicular to both $\boldsymbol{\lambda}$ and $\boldsymbol{\lambda}_i$.

B. Elastica equations for small 3D perturbations

We assume that both perturbations, u , and v , are small and obtain a set of linearized equations. We present the zero-order and first-order equations, and then we consider the spectral problem that gives information about the stability of the perturbations.

Expanding the governing elastica equation (1), one obtains the following zero-order equations,

$$\dot{\phi} = -\sin^2 \phi, \quad (3)$$

$$\dot{\theta} = \frac{1}{4} \sin(2\phi) \sin(2\theta), \quad (4)$$

$$T = -\frac{\eta}{4} \sin^2 \theta \sin(2\phi) \left(s^2 - \frac{1}{4}\right), \quad (5)$$

with the assumed boundary condition $T = 0$ at the ends of the filament, i.e., for $s = \pm \frac{1}{2}$. By solving Eqs (3)-(4), one obtains evolution of the filament orientation,

$$\cot \phi(t) = t + B, \quad (6)$$

$$\tan \theta(t) = \frac{C}{\sin \phi(t)}, \quad (7)$$

where B and C are constants dependent on initial conditions. The zero-order motion of elastica corresponds to the Jeffery orbit [35] in the limit of an infinitely thin rigid rod (the aspect ratio $\ell \rightarrow \infty$). In this limit, the time to approach (or leave) $\phi = 0$ or π is infinite, and therefore an elastica does not tumble, and as such, it can approximate dynamics of a fiber with a non-zero thickness only for the angle ϕ not very close to zero or π [26, 29]. However, Jeffery trajectories $\theta(\phi)$ of the elastica zero-order motion and of a rigid rod with a sufficiently large aspect ratio, e.g. $\ell \gtrsim 100$, are very close to each other, as illustrated in Fig. 2.

Further, the first-order equations are derived from Eq. (1). The in-plane perturbation u satisfies the following equation,

$$u_{ssss} + 2\eta u_t + \eta \sin(2\phi)u + \eta \sin(2\phi) \sin^2 \theta s u_s + \frac{\eta}{4} \sin(2\phi) \sin^2 \theta \left(s^2 - \frac{1}{4}\right) u_{ss} = 0. \quad (8)$$

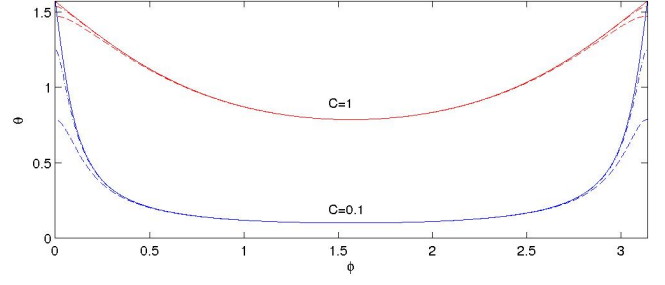


FIG. 2: Jeffery orbits $\theta(\phi)$ in a shear flow for spheroids with the aspect ratios $\ell=10$ (dashed line) and $\ell=30$ (dash-dotted line) [35] and for the zero-order elastica, Eq. (7) (solid line). The corresponding values of C as indicated.

The equation for the out-of-plane perturbation v has the form

$$v_{ssss} + 2\eta v_t - \eta \sin(2\phi) \cos^2 \theta v + 2\eta \cos(2\phi) \cos(\theta) u + \eta \sin(2\phi) \sin^2 \theta s v_s + \frac{\eta}{4} \sin(2\phi) \sin^2 \theta \left(s^2 - \frac{1}{4}\right) v_{ss} = 0. \quad (9)$$

In the considered system, there are no external torques exerted on the filament ends,

$$u_{ss} = v_{ss} = 0 \text{ at } s = \pm \frac{1}{2}, \quad (10)$$

and external forces on the filament ends vanish,

$$u_{sss} = v_{sss} = 0 \text{ at } s = \pm \frac{1}{2}. \quad (11)$$

C. Eigenproblem and stability

To estimate stability of the in-plane (u) and out-of-plane (v) perturbations, we consider the following eigenproblem, which is a 3D generalization of the in-plane study [21], and in the next section will be solved by the Chebyshev spectral collocation method [31, 36], also applied in [12, 21]. We follow the standard assumption that

$$\{u, v\} = \{\Phi_u(s) \exp(\sigma t), \Phi_v(s) \exp(\sigma t)\}, \quad (12)$$

where Φ_u and Φ_v are shapes of the in- and out-of-plane perturbations and σ is the complex growth rate. Then we obtain the following spectral problem,

$$2\eta \left(\sigma + \frac{\sin(2\phi)}{2}\right) \Phi_u = \mathcal{L}[\Phi_u], \quad (13)$$

$$2\eta \left(\sigma - \frac{\sin(2\phi)}{2} \cos^2 \theta\right) \Phi_v = \mathcal{L}[\Phi_v] - 2\eta \cos(2\phi) \cos \theta \Phi_u, \quad (14)$$

where \mathcal{L} denotes the differential operator

$$\mathcal{L} = -\frac{\partial^4}{\partial s^4} - \frac{\eta}{4} \left(s^2 - \frac{1}{4}\right) \sin(2\phi) \sin^2 \theta \frac{\partial^2}{\partial s^2} - \eta s \sin(2\phi) \sin^2 \theta \frac{\partial}{\partial s}, \quad (15)$$

and the boundary conditions follow from Eqs (10)-(11).

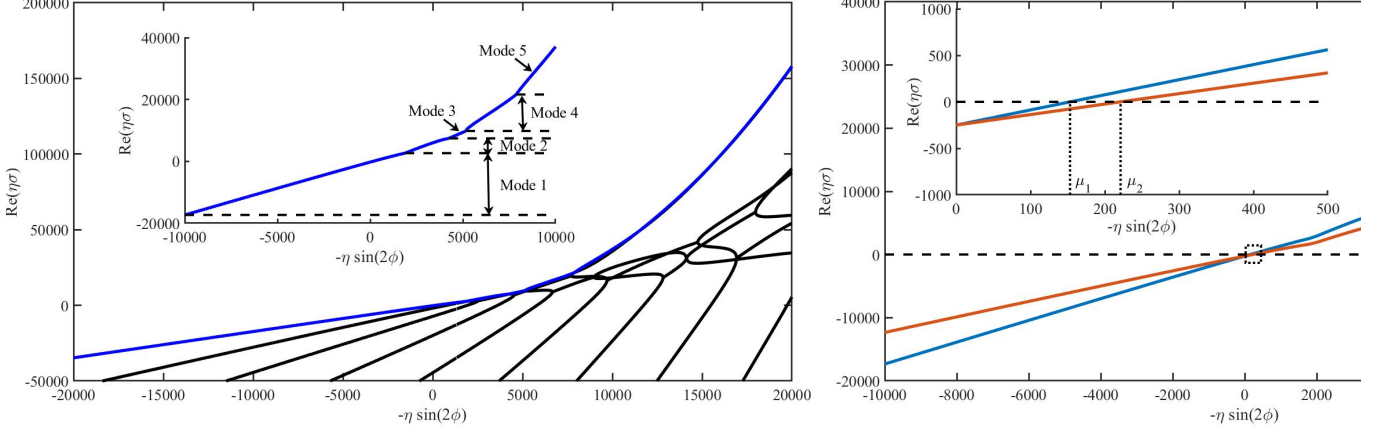


FIG. 3: Left: The real part of the eigenspectrum $\eta\sigma \equiv \eta\sigma_u$, defined in Eqs (16) and (18), as a function of $-\eta \sin(2\phi)$. Right: The largest eigenvalues, $\eta\sigma_u$ and $\eta\sigma_v$, for the in-plane (blue) and out-of-plane (red) perturbations, Φ_u and Φ_v , respectively.

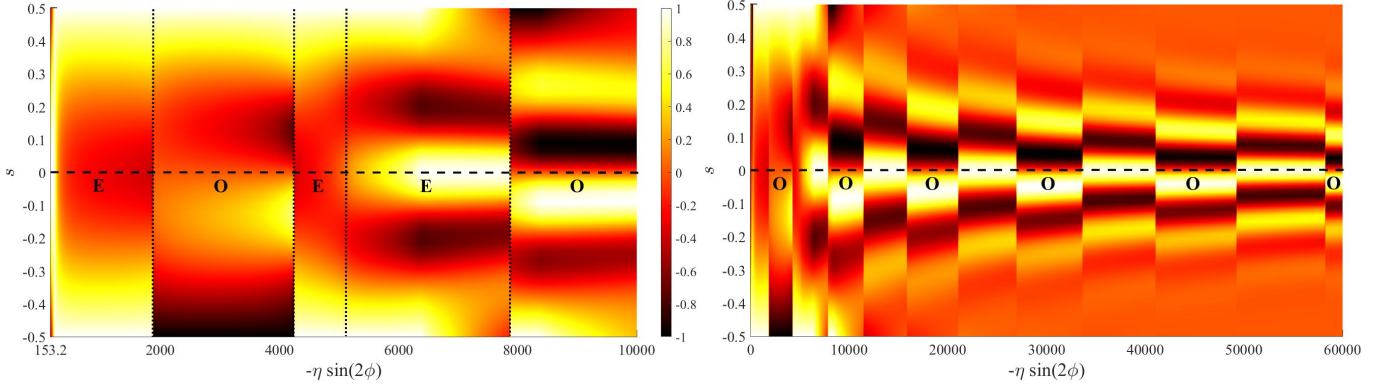


FIG. 4: The most unstable eigenfunctions $\Phi_u(s)$ are even (E) or odd (O), depending on $-\eta \sin(2\phi)$. Colors indicate values of $-1 \leq \Phi_u(s) \leq 1$. Left: the most unstable modes 1-5 in the lowest range of $-\eta \sin(2\phi)$, discussed in Ref. [21]. Right: overview.

III. SPECTRUM AND EIGENFUNCTIONS

We consider the eigenproblem for the in-plane and out-of-plane perturbations when $\theta = \pi/2$. The spectral problem for the in-plane perturbations at $\theta = \pi/2$ was solved by Becker & Shelley [21], who were interested in this special case because for an almost straight elastic filament performing a Jeffery orbit in the plane of shear, i.e. at $\theta = \pi/2$, the hydrodynamic forces exerted on it by the fluid are the largest.

Here we extend the results from Ref. [21] by taking into account not only in-plane, but also out-of-plane perturbations, Φ_u and Φ_v , respectively. In case of $\theta = \pi/2$, the first-order Eqs (13)-(15) for the exponentially growing perturbations (12) have the form,

$$(2\eta\sigma_u + \eta \sin(2\phi))\Phi_u = \tilde{\mathcal{L}}[\Phi_u], \quad (16)$$

$$2\eta\sigma_v\Phi_v = \tilde{\mathcal{L}}[\Phi_v], \quad (17)$$

with

$$\tilde{\mathcal{L}} = -\frac{\partial^4}{\partial s^4} - \frac{\eta \sin(2\phi)}{4} \left(s^2 - \frac{1}{4}\right) \frac{\partial^2}{\partial s^2} - \eta \sin(2\phi) s \frac{\partial}{\partial s}. \quad (18)$$

Eqs (16) and (17) for the in-plane and out-of-plane perturbations decouple from each other. The eigenfunction Φ_u belonging to an eigenvalue σ_u is identical to the eigenfunction Φ_v belonging to the shifted eigenvalue $\sigma_u + \sin(2\phi)/2$. Therefore, we focus on the solutions to Eqs (16) and (18). The generalization for the out-of-plane perturbations is straightforward.

We solve the eigenvalue problem for Φ_u , defined by Eqs (16) and (18), by the Chebyshev spectral collocation method. The calculated eigenspectrum for the in-plane perturbation Φ_u is demonstrated in the left panel of Fig. 3. It agrees well with the result presented in Fig. 2 of Ref. [21]; also, the ranges of $-\eta \sin(2\phi)$ corresponding to modes 1-5 are the same.

The modes 1-5 are the most unstable eigenfunctions Φ_u for the range of the smallest positive eigenvalues σ_u , shown in our Fig. 3 and Fig. 2 of Ref. [21]. The modes 1-5 appear for $153.2 \leq -\eta \sin(2\phi) \leq 10^4$. Their shapes are presented in the left panel of Fig. 4, using colors. The eigenfunctions Φ_u are normalized in such a way that $\max_s(\Phi_u(s)) = 1$. In the right panel of Fig. 4, shapes of the most unstable eigenfunctions Φ_u are shown for the

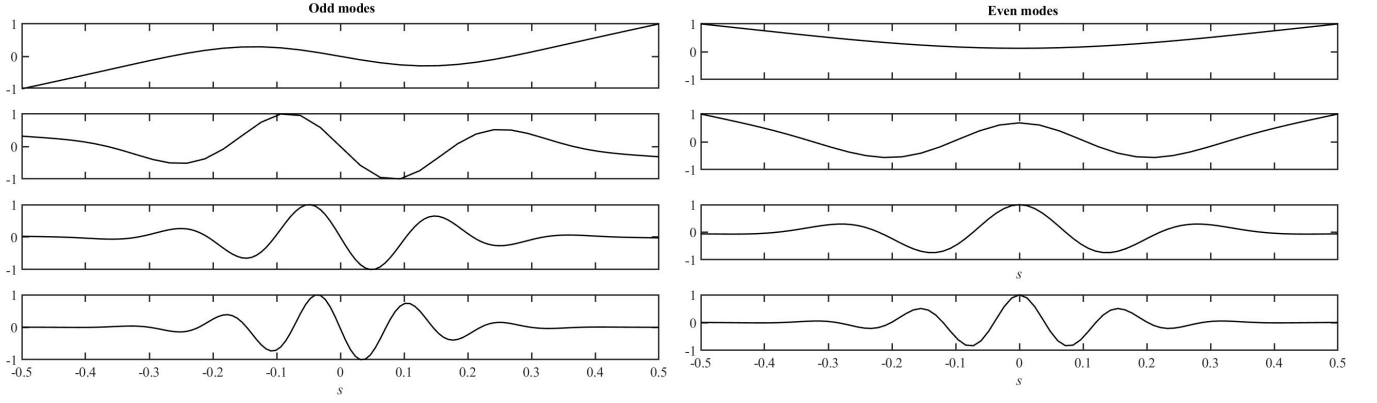


FIG. 5: Examples of the most unstable eigenfunctions $\Phi_u(s)$. Left, top-down: $-\eta \sin(2\phi) = 3000$ (odd mode 2), 10000 (odd mode 5), 30000 and 60000 (higher odd modes). Right, top-down: $-\eta \sin(2\phi) = 300$ (even mode 1), 6000 (even mode 4), 15000 and 50000 (higher even modes).

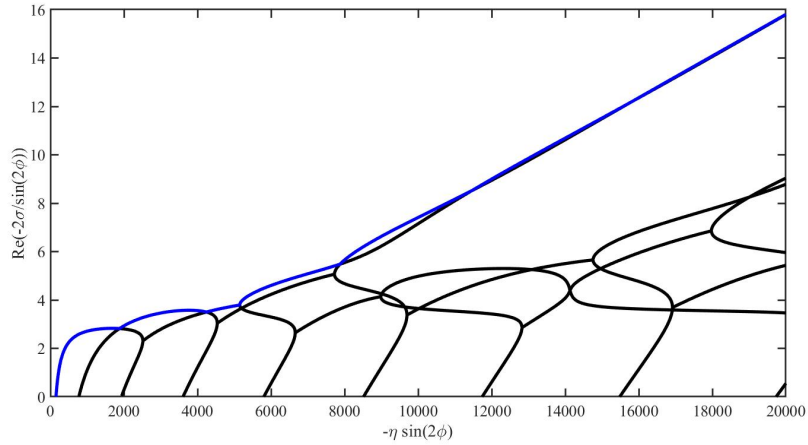


FIG. 6: Scaled eigenspectrum $\sigma = \sigma_u$ for perturbations Φ_u within the shear plane of the shear flow.

whole range $0 \leq -\eta \sin(2\phi) \leq 6 \cdot 10^4$.

The eigenfunctions Φ_u corresponding to the most unstable eigenvalues are even for modes 1, 3, and 4, and odd for modes 2 and 5. In general, for certain values of $-\eta \sin(2\phi)$ they are odd, as in the left panel of Fig. 5; for other values they are even, as in the right panel of Fig. 5. At larger values of $-\eta \sin(2\phi)$, there appear buckling modes with larger wavenumbers. This finding seems to agree with more buckled shapes observed in the numerical simulations with the decreased bending stiffness, as shown in Fig. 12 of Ref. [29].

For stability analysis, the most important are the largest eigenvalues. In the right panel of Fig. 3, the largest eigenvalues for the in-plane and out-of-plane perturbations are compared with each other. The eigenspectrum for Eqs (17) and (18), i.e., for perturbations Φ_v perpendicular to the shear plane, corresponds to $\eta \sigma_v = \eta \sigma_u + \eta \sin(2\phi)/2$. Therefore, the growth rate of the most unstable out-of-plane perturbations is smaller than the growth rate of the most unstable in-plane perturbations, as illustrated in the right panel of Fig. 3. The zeros of the eigenvalues σ_u and σ_v correspond to $-\eta \sin(2\phi) = \mu_1$ and μ_2 , respectively, with $\mu_1 = 153.2$

and $\mu_2 = 221.2$, as shown in the right panel of Fig. 3. This means that the filament with an initial angle ϕ slightly smaller than π , while moving in the shear flow and decreasing the value of ϕ , will first experience in-plane instability, and later out-of-plane instability.

It is very interesting to point out that Eqs (16)-(18) are essentially the same as Eqs (3)-(4) in Ref. [12] for elastica in the compressional ambient flow $\mathbf{u} = (-x, y, 0)$, with the following modifications: instead of $\bar{\mu}$, σ , Φ_y and Φ_z from Ref. [12], here we have $-\eta \sin(2\phi)$, $-2\sigma/\sin(2\phi)$, Φ_u and Φ_v , respectively. Therefore, if we rescale our eigenvalues σ_u by $-\frac{\sin(2\phi)}{2}$, a scaled eigenspectrum is obtained, shown in Fig. 6, which is the same as that illustrated by Chakrabarti *et al.* [12] in their Fig. 3a for their unstable planar eigenspectrum in the compressional flow. The eigenspectra in shear and compressional flows are the same.

When $-\eta \sin(2\phi)$ increases from 153.2 (critical value at which the buckling instability occurs) to 10^4 , there appear even, odd, even, even, and odd modes, respectively. When $-\eta \sin(2\phi)$ increases above 10^4 , the most unstable mode still keeps alternating odd and even symmetries.

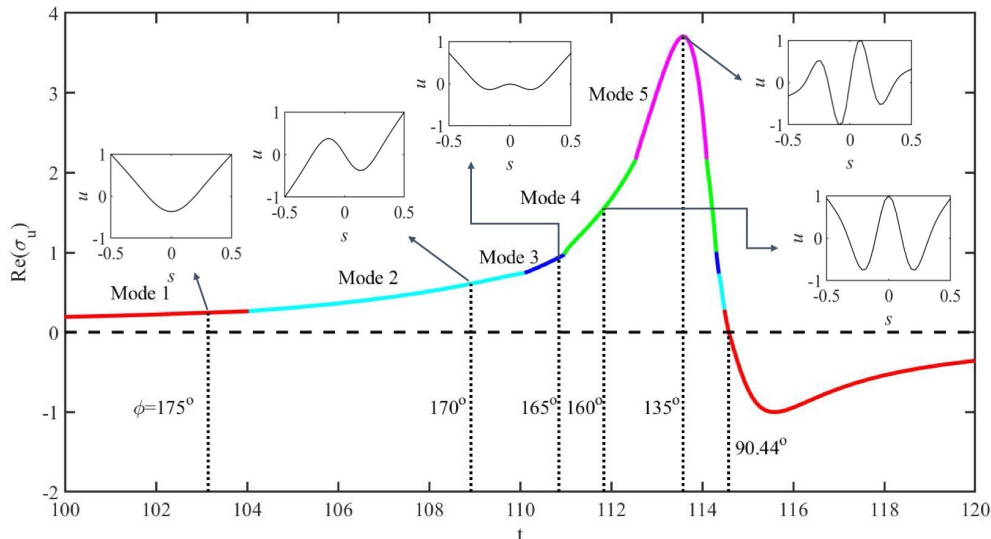


FIG. 7: Spectral problem for elastica evolving in time t according to the zero-order Eqs (6), assuming that elastica is straight with a very small perturbation only. The real part of the most unstable eigenvalue σ_u (in-plane perturbations) for different orientations λ of almost straight elastica with $\eta = 10000$. Here $\theta = \pi/2$ and ϕ decreases with time from $\phi_0 = 179.5^\circ$ at $t = 0$. The corresponding most unstable eigenfunctions are also shown.

This coupling of the even and odd most unstable modes was described and shown in Fig. 3 in Ref. [12] in the context of the compressional flow.

The spectral analysis provides the growth rate of small perturbations, given by Eq. (12), with the amplitudes independent of time. Keeping it in mind, in Fig. 7 we illustrate how the most unstable eigenfunctions and eigenvalues change when the filament is almost straight and its orientation λ is changed according to the zeroth order Eqs (6)-(7). In particular, as expected, the fastest growth of small perturbations is observed for $\phi = 135^\circ$. The unstable perturbations correspond only to angles ϕ larger than 90° plus a certain small value. Fig. 7 shows that the shapes and parity of the most unstable eigenfunctions are different for different orientations, for the same value of η .

IV. CONCLUSIONS

In this work, we derived Eqs (8)-(9) for the evolution of 3-dimensional perturbations of a straight elastica at an

arbitrary orientation. We performed spectral analysis of elastica in a shear flow, investigating perturbations out of the shear plane. We analyzed the most unstable eigenfunctions and eigenvalues. We demonstrated that the eigenproblem for elastica in the shear flow is described by the same equations as in the compressional flow [12].

Based on the spectral analysis presented here, in Ref. [37] scaling law for the eigenfunction shape has been derived and compared with the numerical simulations of flexible filaments made of beads. In the future, it would be interesting to extend the spectral analysis presented here and in Ref. [37] for an elastic sheet in a shear flow. Such a system has been recently studied, e.g., in Refs [38–42], with potential applications for graphene flakes.

Acknowledgements

M. L. E.-J. thanks Prof. Howard A. Stone and Dr. Piotr Zdybel for helpful discussions. This work was supported in part by the National Science Centre under grant UMO-2018/31/B/ST8/03640.

-
- [1] A. Lindner and M. J. Shelley, “Elastic fibers in flows,” in *Fluid-Structure Interactions in Low Reynolds Number Flows* (C. Duprat and H. A. Stone, eds.), pp. 168–189, Royal Society of Chemistry, 2015.
 - [2] O. Du Roure, A. Lindner, E. N. Nazockdast, and M. J. Shelley, “Dynamics of flexible fibers in viscous flows and fluids,” *Annu. Rev. Fluid Mech.*, vol. 51, pp. 539–572, 2019.
 - [3] T. A. Witten and H. Diamant, “A review of shaped colloidal particles in fluids: anisotropy and chirality,” *Rep. Prog. Phys.*, vol. 83, no. 11, p. 116601, 2020.
 - [4] H. Nguyen and L. Fauci, “Hydrodynamics of diatom chains and semiflexible fibres,” *J. R. Soc. Interface*, vol. 11, no. 96, p. 20140314, 2014.
 - [5] V. Kantsler and R. E. Goldstein, “Fluctuations, dynamics, and the stretch-coil transition of single actin filaments in extensional flows,” *Phys. Rev. Lett.*, vol. 108, no. 3, p. 038103, 2012.

- [6] K. Sinha and M. D. Graham, “Dynamics of a single red blood cell in simple shear flow,” *Phys. Rev. E*, vol. 92, no. 4, p. 042710, 2015.
- [7] M. Harasim, B. Wunderlich, O. Peleg, M. Kröger, and A. R. Bausch, “Direct observation of the dynamics of semiflexible polymers in shear flow,” *Phys. Rev. Lett.*, vol. 110, no. 10, p. 108302, 2013.
- [8] Y. Liu, B. Chakrabarti, D. Saintillan, A. Lindner, and O. Du Roure, “Morphological transitions of elastic filaments in shear flow,” *P. Natl. Acad. Sci. US*, vol. 115, no. 38, pp. 9438–9443, 2018.
- [9] J. K. Nunes, H. Constantin, and H. A. Stone, “Microfluidic tailoring of the two-dimensional morphology of crimped microfibers,” *Soft Matter*, vol. 9, no. 16, pp. 4227–4235, 2013.
- [10] P. Nakielski, S. Pawłowska, F. Pierini, W. Liwińska, P. Hejduk, K. Zembrzycki, E. Zabost, and T. A. Kowalewski, “Hydrogel nanofilaments via core-shell electrospinning,” *PLoS One*, vol. 10, no. 6, p. e0129816, 2015.
- [11] H. Manikantan and D. Saintillan, “Buckling transition of a semiflexible filament in extensional flow,” *Phys. Rev. E*, vol. 92, no. 4, p. 041002, 2015.
- [12] B. Chakrabarti, Y. Liu, J. LaGrone, R. Cortez, L. Fauci, O. du Roure, D. Saintillan, and A. Lindner, “Flexible filaments buckle into helicoidal shapes in strong compressional flows,” *Nat. Phys.*, pp. 1–6, 2020.
- [13] Y.-N. Young and M. J. Shelley, “Stretch-coil transition and transport of fibers in cellular flows,” *Phys. Rev. Lett.*, vol. 99, no. 5, p. 058303, 2007.
- [14] E. Wandersman, N. Quennou, M. Fermigier, A. Lindner, and O. Du Roure, “Buckled in translation,” *Soft Matter*, vol. 6, no. 22, pp. 5715–5719, 2010.
- [15] N. Quennou, M. Shelley, O. Du Roure, and A. Lindner, “Transport and buckling dynamics of an elastic fibre in a viscous cellular flow,” *J. Fluid Mech.*, vol. 769, pp. 387–402, 2015.
- [16] Q. Yang and L. Fauci, “Dynamics of a macroscopic elastic fibre in a polymeric cellular flow,” *J. Fluid Mech.*, vol. 817, pp. 388–405, 2017.
- [17] L. Guglielmini, A. Kushwaha, E. S. G. Shaqfeh, and H. A. Stone, “Buckling transitions of an elastic filament in a viscous stagnation point flow,” *Phys. Fluids*, vol. 24, no. 12, p. 123601, 2012.
- [18] N. Autrusson, L. Guglielmini, S. Lecuyer, R. Rusconi, and H. A. Stone, “The shape of an elastic filament in a two-dimensional corner flow,” *Phys. Fluids*, vol. 23, no. 6, p. 063602, 2011.
- [19] O. L. Forgacs and S. G. Mason, “Particle motions in sheared suspensions IX. Spin and deformation of threadlike particles,” *J. Coll. Sci. Imp. U. Tok.*, vol. 14, no. 5, pp. 457–472, 1959.
- [20] O. L. Forgacs and S. G. Mason, “Particle motions in sheared suspensions: X. Orbits of flexible threadlike particles,” *J. Coll. Sci. Imp. U. Tok.*, vol. 14, no. 5, pp. 473–491, 1959.
- [21] L. E. Becker and M. J. Shelley, “Instability of elastic filaments in shear flow yields first-normal-stress differences,” *Phys. Rev. Lett.*, vol. 87, no. 19, p. 198301, 2001.
- [22] C. Kurzthaler, R. Brandão, O. Schnitzer, and H. A. Stone, “Shape of a tethered filament in various low-Reynolds-number flows,” *Phys. Rev. Fluids*, vol. 8, p. 014101, 2023.
- [23] A. M. Słowicka, E. Wajnryb, and M. L. Ekiel-Jeżewska, “Dynamics of flexible fibers in shear flow,” *J. Chem. Phys.*, vol. 143, no. 12, p. 124904, 2015.
- [24] J. LaGrone, R. Cortez, W. Yan, and L. Fauci, “Complex dynamics of long, flexible fibers in shear,” *J. Nonnewton. Fluid Mech.*, vol. 269, pp. 73–81, 2019.
- [25] M. Kanchan and R. Maniyeri, “Numerical simulation and prediction model development of multiple flexible filaments in viscous shear flow using immersed boundary method and artificial neural network techniques,” *Fluid Dyn. Res.*, vol. 52, no. 4, p. 045507, 2020.
- [26] A. M. Słowicka, H. A. Stone, and M. L. Ekiel-Jeżewska, “Flexible fibers in shear flow approach attracting periodic solutions,” *Phys. Rev. E*, vol. 101, no. 2, p. 023104, 2020.
- [27] P. J. Żuk, A. M. Słowicka, M. L. Ekiel-Jeżewska, and H. A. Stone, “Universal features of the shape of elastic fibres in shear flow,” *J. Fluid Mech.*, vol. 914, p. A31, 2021.
- [28] N. Xue, J. K. Nunes, and H. A. Stone, “Shear-induced migration of confined flexible fibers,” *Soft Matter*, vol. 18, no. 3, pp. 514–525, 2022.
- [29] A. M. Słowicka, N. Xue, P. Sznajder, J. K. Nunes, H. A. Stone, and M. L. Ekiel-Jeżewska, “Buckling of elastic fibers in a shear flow,” *New J. Phys.*, vol. 24, no. 1, p. 013013, 2022.
- [30] F. Bonacci, B. Chakrabarti, D. Saintillan, O. Du Roure, and A. Lindner, “Dynamics of flexible filaments in oscillatory shear flows,” *J. Fluid Mech.*, vol. 955, p. A35, 2023.
- [31] L. N. Trefethen, “Chebyshev differentiation matrices,” in *Spectral methods in Matlab*, pp. 51–59, SIAM, Philadelphia, 2000.
- [32] G. Batchelor, “Slender-body theory for particles of arbitrary cross-section in Stokes flow,” *J. Fluid Mech.*, vol. 44, no. 3, pp. 419–440, 1970.
- [33] B. Audoly and Y. Pomeau, “Elasticity and geometry,” in *Peyresq Lectures On Nonlinear Phenomena*, pp. 1–35, World Scientific, 2000.
- [34] B. Audoly, “Introduction to the elasticity of rods,” in *Fluid-Structure Interactions in Low-Reynolds-Number Flows* (C. Duprat and H. A. Stone, eds.), pp. 1–24, Royal Society of Chemistry, 2015.
- [35] M. D. Graham, *Microhydrodynamics, Brownian motion, and complex fluids*, vol. 58. Cambridge University Press, 2018.
- [36] J. P. Boyd, “Interpolation, collocation & all that,” in *Chebyshev and Fourier spectral methods*, pp. 81–97, DOVER, New York, 2001.
- [37] P. Sznajder, L. Liu, P. Zdybel, and M. L. Ekiel-Jeżewska, “Scaling law for a buckled elastic filament in a shear flow,” <https://arxiv.org>, 2023.
- [38] M. J. Shelley and J. Zhang, “Flapping and bending bodies interacting with fluid flows,” *Annual Review of Fluid Mechanics*, vol. 43, pp. 449–465, 2011.
- [39] Y. Xu and M. J. Green, “Brownian dynamics simulations of nanosheet solutions under shear,” *J. Chem. Phys.*, vol. 141, no. 2, p. 024905, 2014.
- [40] Y. Yu and M. D. Graham, “Coil-stretch-like transition of elastic sheets in extensional flows,” *Soft Matter*, vol. 17, no. 3, pp. 543–553, 2021.
- [41] K. S. Silmore, M. S. Strano, and J. W. Swan, “Buckling, crumpling, and tumbling of semiflexible sheets in simple shear flow,” *Soft Matter*, vol. 17, no. 18, pp. 4707–4718, 2021.
- [42] G. Salussolia, C. Kamal, J. Stafford, N. Pugno, and L. Botto, “Simulation of interacting elastic sheets in

shear flow: Insights into buckling, sliding, and reassembly of graphene nanosheets in sheared liquids,” *Physics*

of Fluids, vol. 34, no. 5, p. 053311, 2022.